doi:10.1093/brain/awx306 BRAIN 2018: 141; 117–131 | 117

BRAIN
A JOURNAL OF NEUROLOGY

A fingerprint of the epileptogenic zone in human epilepsies

Olesya Grinenko,[1]* Jian Li,[2]* John C. Mosher,[1] Irene Z. Wang,[1] Juan C. Bulacio,[1] Jorge Gonzalez-Martinez,[1] Dileep Nair,[1] Imad Najm,[1] Richard M. Leahy[2] and Patrick Chauvel[1]

*These authors contributed equally to this work.

Defining a bio-electrical marker for the brain area responsible for initiating a seizure remains an unsolved problem. Fast gamma activity has been identified as the most specific marker for seizure onset, but conflicting results have been reported. In this study, we describe an alternative marker, based on an objective description of interictal to ictal transition, with the aim of identifying a time-frequency pattern or 'fingerprint' that can differentiate the epileptogenic zone from areas of propagation. Seventeen patients who underwent stereoelectroencephalography were included in the study. Each had seizure onset characterized by sustained gamma activity and were seizure-free after tailored resection or laser ablation. We postulated that the epileptogenic zone was always located inside the resection region based on seizure freedom following surgery. To characterize the ictal frequency pattern, we applied the Morlet wavelet transform to data from each pair of adjacent intracerebral electrode contacts. Based on a visual assessment of the time-frequency plots, we hypothesized that a specific time-frequency pattern in the epileptogenic zone should include a combination of (i) sharp transients or spikes; preceding (ii) multiband fast activity concurrent; with (iii) suppression of lower frequencies. To test this hypothesis, we developed software that automatically extracted each of these features from the time-frequency data. We then used a support vector machine to classify each contact-pair as being within epileptogenic zone or not, based on these features. Our machine learning system identified this pattern in 15 of 17 patients. The total number of identified contacts across all patients was 64, with 58 localized inside the resected area. Subsequent quantitative analysis showed strong correlation between maximum frequency of fast activity and suppression inside the resection but not outside. We did not observe significant discrimination power using only the maximum frequency or the timing of fast activity to differentiate contacts either between resected and non-resected regions or between contacts identified as epileptogenic versus non-epileptogenic. Instead of identifying a single frequency or a single timing trait, we observed the more complex pattern described above that distinguishes the epileptogenic zone. This pattern encompasses interictal to ictal transition and may extend until seizure end. Its time-frequency characteristics can be explained in light of recent models emphasizing the role of fast inhibitory interneurons acting on pyramidal cells as a prominent mechanism in seizure triggering. The pattern clearly differentiates the epileptogenic zone from areas of propagation and, as such, represents an epileptogenic zone 'fingerprint'.

1 Epilepsy Center, Cleveland Clinic Neurological Institute, Cleveland OH, USA
2 Signal and Image Processing Institute, University of Southern California, Los Angeles CA, USA

Correspondence to: Patrick Chauvel
Epilepsy Center, Cleveland Clinic Neurological Institute, 9500 Euclid Avenue, Cleveland OH 44195, USA
E-mail: chauvep@ccf.org

Keywords: epilepsy surgery; epileptogenic zone; high-frequency oscillations; stereo-EEG; imaging methodology

Abbreviations: SEEG = stereo-electro-encephalography; SVM = support vector machine

Received June 7, 2017. Revised September 21, 2017. Accepted September 27, 2017. Advance Access publication December 14, 2017
© The Author (2017). Published by Oxford University Press on behalf of the Guarantors of Brain.
This is an Open Access article distributed under the terms of the Creative Commons Attribution Non-Commercial License (http://creativecommons.org/licenses/by-nc/4.0/), which permits non-commercial re-use, distribution, and reproduction in any medium, provided the original work is properly cited. For commercial re-use, please contact journals.permissions@oup.com

Downloaded from https://academic.oup.com/brain/article-abstract/141/1/117/4746664
by guest
on 08 January 2018

Introduction

The epileptogenic zone, defined as the site of primary organization of ictal discharge, refers to the areas bound together through an excessive synchronization at seizure onset (Bancaud *et al.*, 1970; Wendling *et al.*, 2010). 'Fast' or 'rapid' activity at ictal onset has been recognized as the main feature of epileptogenic zone since the infancy of stereotactically-implanted intracranial EEG (SEEG) electrodes (Bancaud and Talairach, 1965). Since the development of subdural electrocorticography (ECoG) recordings, much attention has also been paid to the time precedence of phasic transients, especially spiking activities (Palmini *et al.*, 1995; Boonyapisit *et al.*, 2003). In the past 15 years, identification of high frequency oscillations during interictal and ictal periods in experimental models reoriented research interest towards high-gamma activities in human epilepsies as a potential epileptogenic zone marker (Bragin *et al.*, 2002; Zijlmans *et al.*, 2012; Matsumoto *et al.*, 2013; Weiss *et al.*, 2016). In parallel, DC recordings exemplified the concomitance of ultra-slow and fast frequencies (Ikeda *et al.*, 1996; Gnatkovsky *et al.*, 2014; Wu *et al.*, 2014; Thompson *et al.*, 2016). Fast activity frequently occurs quasi-simultaneously in multiple areas so that visual discrimination can be cumbersome and lead to subjective interpretations. Several methods of objective localization of the epileptogenic zone based on ictal SEEG signal processing have been developed during the past 10 years. Bartolomei *et al.* (2008) measured the relative onset times of changes in energy ratio between fast and slow activities in different areas involved at seizure onset to define an epileptogenicity index. David *et al.* (2011) mapped the anatomical location of the fastest activities and their slow propagation during peri-onset time onto the patients' MRIs and compared the location with the surgical resection area. A different approach, frequency localization, was used by Gnatkovsky *et al.* (2011). After defining frequencies of interest and plotting their power change over time, they localized the distribution of frequencies of interest in different contacts of the depth electrodes. The epileptogenic zone, defined as the area exhibiting frequency changes at seizure onset, could then be delineated. In a retrospective and prospective study of patients investigated using SEEG, the same method was applied to test three potential biomarkers of epileptogenic zone, namely fast activity, signal flattening and slow potential shift. These biomarkers co-localized with the epileptogenic zone as defined by standard SEEG criteria and post-resection seizure outcome (Gnatkovsky *et al.*, 2014).

Differentiating the primary epileptogenic zone from regions of propagation is difficult using fast activity signal analysis. In practice, fast frequencies and their time of occurrence can be easily identified in temporal lobe seizures (Bartolomei *et al.*, 2008); however, a degree of epileptogenicity cannot be similarly defined in neocortical epilepsies, where these changes occur abruptly and simultaneously over widespread cortical areas. Furthermore, if the highest frequency is an indicator of the most epileptogenic areas, it is not clear whether lower frequencies would mark less or non-epileptogenic ones. Failures in epilepsy surgery for focal cortical dysplasia are often due to difficulty in estimating the extent of fast activity-generating cortex to be removed for a seizure-free outcome (Aubert *et al.*, 2009).

Depending on the region involved and/or the underlying pathology, fast activity may be preceded by or emerge from a sharp wave or rhythmical high-amplitude spiking (Spencer *et al.*, 1992; Palmini *et al.*, 1995; Lagarde *et al.*, 2016). Seizure onset is not a monomorphic but a complex phenomenon. Characterization of the significance of fast activity cannot be appraised in isolation.

A holistic approach is absent from the literature, motivating us to objectively describe interictal/pre-ictal/ictal transition and ictal evolution using time-frequency analysis applied to all electrodes in patients undergoing SEEG. After qualitatively identifying a time-frequency pattern only present in the epileptogenic zone, we developed a support vector machine (SVM)-based learning system to distinguish time-frequency patterns inside the epileptogenic zone from those outside the epileptogenic zone and demonstrated its effectiveness. This pattern lasts for a period of time and is beyond strict seizure onset and it can differentiate the epileptogenic zone from areas of propagation. Characterized by combined variations in high and low frequencies, possibly reflecting changes in neuronal unit activities like those reported using simultaneous ECoG and microelectrode unit recordings (Weiss *et al.*, 2013, 2015; Truccolo *et al.*, 2014; Merricks *et al.*, 2015), the time-frequency pattern we describe represents an epileptogenic zone 'fingerprint'.

Patients and materials

Patient selection and data collection

Working under an Institutional Review Board approved protocol at the Cleveland Clinic, we included 17 patients who underwent SEEG evaluation in our Epilepsy Centre. Our inclusion criteria were: (i) tailored resection or laser ablation guided by SEEG; (ii) three or more seizures recorded during SEEG that were characterized by sustained (3-s duration or longer) gamma activity at the onset; (iii) no seizures, including auras, after surgery. Details of the patient selection protocol are presented Supplementary material, section 1.

The SEEG evaluation was a clinically determined invasive presurgical modality for patients with pharmaco-resistant focal epilepsy, incongruent non-invasive data, or a negative MRI with the absence of a clear epileptogenic lesion. Anatomo-electroclinical hypotheses were formulated individually for each patient during a multidisciplinary patient management conference based on available non-invasive data: clinical history, video EEG, MRI, PET, ictal

Downloaded from https://academic.oup.com/brain/article-abstract/141/1/117/4746664
by guest
on 08 January 2018

single-photon emission computed tomography and MEG. SEEG implantation was performed using multi-lead depth electrodes (AdTech, Integra, or PMT). The electrodes were implanted according to the Talairach stereotactic method using orthogonal or oblique trajectories (Gonzalez-Martinez *et al.*, 2014).

Anatomical locations of the electrode leads were checked by the digital fusion of a post-implantation thin-sliced CT 3D image with a preoperative T_1-weighted volumetric MRI. Images were aligned and verified using CURRY 7 (Compumedics NeuroScan). The SEEG signals were recorded on Nihon Kohden EEG system with a sampling rate of 500 Hz (until 2012, seven patients in our study) or 1000 Hz (2012 and later, 10 patients). After the SEEG evaluation, patients underwent a tailored resection, or a laser ablation of the identified epileptogenic zone. A post-operative MRI was acquired 1–6 months after surgery, aligned to the CT, and used to identify electrode contacts that were positioned in the resected/ablated area.

Follow-up information was collected from a review of the medical records. We also collected retrospective data about age of epilepsy onset and epilepsy duration, localization and type of lesion based on MRI, surgical neuropathology, and resection details. Seventeen patients matched inclusion criteria. All patients were seizure free with a mean follow up duration of 42.9 months [standard deviation (SD) 20.4 months]. Table 1 shows the clinical profiles of these patients.

Data selection and time-frequency decomposition

Three typical clinical seizures characterized by sustained gamma band activity at the onset were selected for each patient. Sixteen patients had a single stereotypical ictal pattern. One patient had two distinct ictal patterns; both patterns were included in the analysis.

For each identified seizure onset, we extracted a window of 40 s of SEEG data: 20 s before and 20 s after the seizure onset. We also collected 40 s of baseline SEEG data 2 min before the seizure onset to use as a statistical baseline for the seizure. All analyses were based on bipolar signals formed as the difference between pairs of adjacent contacts on each electrode. Channels containing visually obvious artefacts were removed.

Two variations of complex Morlet wavelet transform (MWT) were applied to each channel of data. For the visual assessment, we used Brainstorm (Tadel *et al.*, 2011) to generate MWTs evaluated at 50 frequencies spaced on a logarithmic scale from 1 to 200 Hz. The Morlet time-frequency index was set to five (i.e. five wavelengths full-width at half-maximum at a given frequency). We used Brainstorm's 'flattening' option, which amplifies the higher frequencies to compensate for the '1/f' characteristic of the power spectrum and gives a more visually appealing image. An example of this processing is shown in Fig. 1. For the automated processing discussed in the 'Feature extraction' section below, the second MWT variation used linear spacing in the frequency range of 1 to 200 Hz with interval 1 Hz, and a Morlet time-frequency index of eight. The baseline SEEG data were processed identically, and the baseline MWT were used to normalize the seizure data MWTs by dividing the power in each frequency line by its baseline power (Supplementary material, section 4).

Visual characteristics of the epileptogenic zone

For each patient in Table 1, we computed time-frequency maps of each SEEG contact, both inside and outside the epileptogenic zone. We show one such exemplar map in Fig. 1B for all contacts in a single patient and, in Fig. 1A, the corresponding SEEG time series for this patient.

Despite the variation in anatomical locations of the epileptogenic zone and the type of epileptogenic lesion from patient to patient, a characteristic time-frequency pattern emerged for contacts located inside epileptogenic zone. Figure 2 shows a typical example of this pattern. At seizure onset, we observed three predominant features from the time frequency map as illustrated in Fig. 2B: (i) single or multiple pre-ictal sharp transient(s) or spike(s) (depending on their slow component duration); (ii) narrow frequency bands of fast activity; with (iii) simultaneous suppression of slow pre-ictal frequencies. The comparison between channels that were localized inside versus outside resection regions revealed the predominance of this pattern inside resected regions (Fig. 1B).

Pre-ictal spikes and sharp transients appeared as either a burst of pre-ictal spikes, or as a single spike. These spikes were characterized by two components, a slow (~delta to theta) activity, and a simultaneous fast activity (high frequency oscillations) in a frequency range from 60 to 200 Hz. These pre-ictal spikes or sharp transients were part of the pattern in 49 of 51 seizures. In the other two seizures, the transient was missing at ictal onset, only a delta burst was observed. The duration of pre-ictal spiking preceding the seizure onset varied in length from a single sharp transient to continuous spiking without clear interictal/pre-ictal transition.

The second notable feature was the narrow-band fast activity, characterized by two or three (four in one case) high-intensity bands (Fig. 2B). The median of maximum frequency of fast activity was 97 Hz [interquartile range (IQR) 33 Hz] across all contacts expressing the characteristic time-frequency pattern and the median of minimum frequency of fast activity was 43 Hz (IQR 21 Hz) (for statistics, see Supplementary Fig. 3). The transition from spikes to fast activity was immediate: either narrow band fast activity appeared right after the last spike (seven patients) or fast activity initially appeared across a broad band of frequencies and then in 1 to 5 s it is organized into several

Downloaded from https://academic.oup.com/brain/article-abstract/141/1/117/4746664
by guest
on 08 January 2018

Table 1 Clinical characteristics of the included patients

Subject ID	Age (years)	Epilepsy duration (years)	MRI lesion	Resection (or ablation) details	Surgical pathology	Follow-up duration (months)[a]	Outcome	Anatomical location of the epileptogenic zone
1	43	37	FCD, insular/frontal operculum	Anterior insula/frontal operculum	FCD, type 2B	13	Seizure-free	Insular/frontal operculum
2	29	22	Negative	Temporal-parietal-occipital	FCD, type 1C	49	Seizure-free	Occipito-temporal
3	33	17	Hippocampal sclerosis	Anterior temporal lobe	Hippocampal sclerosis type 1	48	Seizure-free	Temporal
4	17	8	Negative	Laser ablation, superior frontal gyrus	No pathology	19	Seizure-free	Frontal
5	16	1	Benign neoplasm, posterior parahippocampal gyrus	Posterior parahippocampus gyrus and neoplasm	Low grade glial/glioneuronal neoplasm	39	Seizure-free	Basal posterior temporal
6	46	41	FCD, mesial frontal	Prefrontal lobe	Non-specific changes	38	Seizure-free	Frontal
7	5	1	Negative	Superior frontal gyrus, superior frontal sulcus, frontal pole	FCD, type 2B	21	Seizure-free	Superior frontal gyrus/superior frontal sulcus
8	63	14	Negative	Orbitofrontal	FCD, type 1	44	Seizure-free	Orbitofrontal/pars orbitalis
9	33	19	Gliotic postop changes	Anterior temporal lobe	FCD, type 1B	40	Seizure-free	Temporal
10	21	11	Negative	Occipital lobe	Grey matter heterotopia, FCD type 1B	12	Seizure-free	Cuneus
11	32	27	FCD, precentral gyrus	Precentral gyrus	Non conclusive	77	Seizure-free	Precentral gyrus
12	22	3	FCD, superior frontal sulcus	Superior and middle frontal gyri, anterior cingulate	FCD type 2 B	78	Seizure-free	Frontal
13	19	18	Negative	Middle frontal gyrus	FCD type 1	48	Seizure-free	Inferior frontal sulcus/middle frontal gyrus
14	30	18	Negative	Frontal operculum	FCD type 2 B	47	Seizure-free	Frontal operculum/subcentral region
15	20	11	Negative	Frontal lobe	FCD, type 1	82	Seizure-free	Superior frontal gyrus/superior frontal sulcus
16	65	25	Negative	Anterior temporal lobe	FCD, 1C	39	Seizure-free	Temporal
17	65	9	Negative	Anterior temporal lobe	FCD, 1C	36	Seizure-free	Temporal

[a]Follow-up information current as of July 2017.
FCD = focal cortical dysplasia.

narrow bands (10 patients). For examples of the variation of the transition, see Supplementary Fig. 2.

The initial fast activity was often associated with a brief increase of activities in some low frequencies, e.g. the delta/theta range. Two other key features of the fast activity were a decreasing frequency shift (also known as 'down-chirping') with the progression of the seizure, and a pulsing amplitude change. The multiple bands were generally not harmonically related; rather, they chirped at different frequencies, pulsed in their own amplitudes independently. In five patients narrow bands of fast activity persisted through the full seizure and ended with a brief burst of spikes. In the rest of the patients, narrow band fast activity transitioned into rhythmical ictal spikes. The maximum duration of the fast activity, as observed over all contacts for a patient, varied from 3 to 91 s (median 15).

Of 17 patients, fast activity appeared simultaneously both inside and outside the resected area in 11 patients;

Downloaded from https://academic.oup.com/brain/article-abstract/141/1/117/4746664
by guest
on 08 January 2018

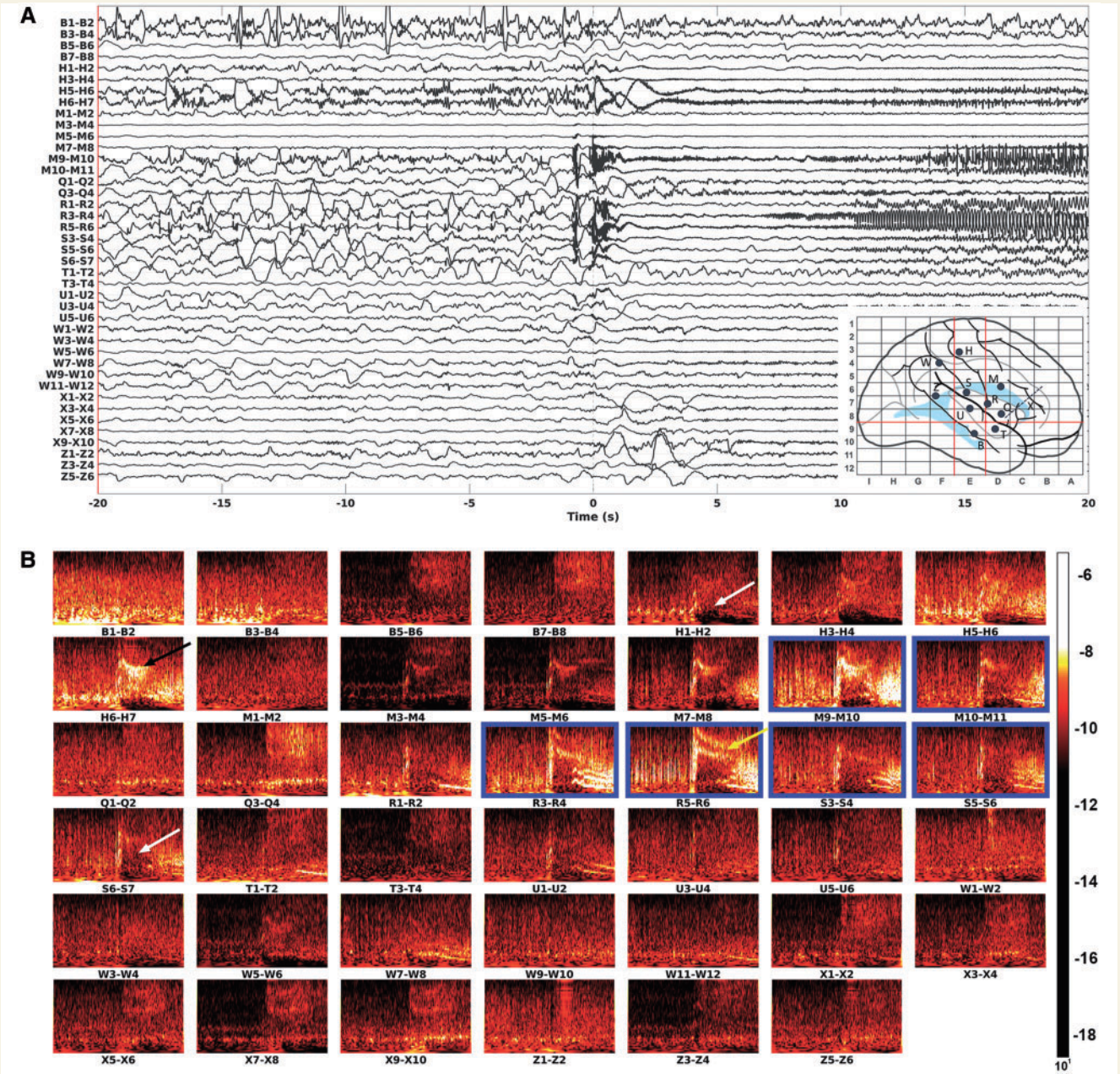

Figure 1 SEEG recording and time-frequency plots of seizure onset. (**A**) The SEEG time series. Bipolar montage was applied by taking the difference between signals from two adjacent contacts. Ictal onset is marked as '0', full duration of the segment is 40 s (from −20 s to 20 s). (**B**) The Morlet time frequency maps corresponding to each bipolar contact pair in **A**. Each graph shows 20 s before the seizure onset to 20 s after the seizure onset, along the horizontal axis. The vertical axis represents frequencies from 1 Hz to 200 Hz, logarithmically spaced and spectrally flattened to emphasize the higher frequencies. Contacts in the resected area are outlined in blue. The pattern characterized by the combination of a spike, multiband fast activity and suppression is localized inside the resected area (yellow arrow), while broadband fast activity (black arrow) and suppression without sustained fast activity (white arrow) are localized outside the resected area.

four patients also had fast activity both inside and outside the resected area but there was a delay from inside to outside that ranged from 100 ms to 3 s; in the remaining two patients, fast activity was observed only inside the resected area.

Fast activity outside the resection area frequently appeared only as a single and broad band of frequencies (Fig. 1B, black arrow). The median of the maximum frequency of fast activity across all contacts outside the resection area was 74 Hz (IQR 28 Hz) and median of the minimum frequency was 44 Hz (IQR 22 Hz) (Supplementary Fig. 3).

The third notable feature was the suppression of low-frequency pre-ictal activity at seizure onset (a decrease of

Downloaded from https://academic.oup.com/brain/article-abstract/141/1/117/4746664
by guest
on 08 January 2018

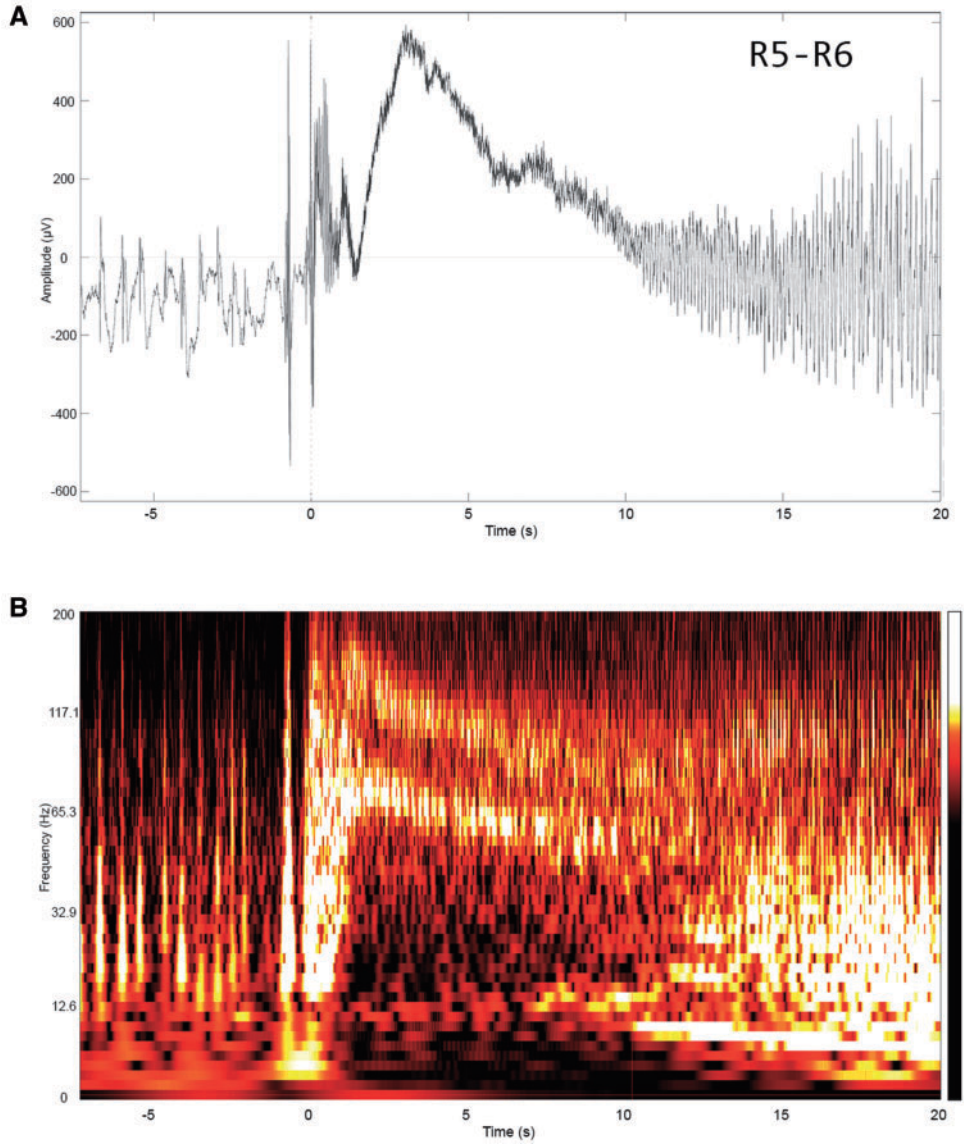

Figure 2 Example of pre-ictal to ictal transitions in the epileptogenic zone. Channel R5-R6 from Fig. 1A from 5 s before to 20 s after the ictal onset is shown in (**A**) and the corresponding time frequency plot (logarithmic scale) is shown in **B**. The time frequency plot shows the proposed 'fingerprint': a combination of pre-ictal spikes, multi-band fast activity and simultaneous suppression of slower background frequencies. Note that fast activity is characterized by multiple bands that are not harmonically related, chirp at different frequency rates, and whose amplitudes vary independently across bands.

signal power in the lower frequencies in the time-frequency plots), which appeared simultaneously with the fast activity (Fig. 2B). The suppression was always most pronounced in the delta-theta frequencies but commonly extended up to gamma frequency range. The median of the maximum frequencies that suppressed across all contacts expressing the pattern was 45 Hz (IQR 20 Hz) (Supplementary Fig. 4). The duration of the suppression was related to the duration of the fast activity, with the suppression often terminated by a burst of intense slow activity, as the fast activity decreased or arrested. Suppression was also observed in the contacts outside the resection, but it was also less intense, more diffuse, and uncorrelated with the fast activity (Fig. 1B, white arrow). The median of the maximum frequencies that suppressed across all contacts outside the resection was 25 Hz (IQR 22 Hz) (Supplementary Fig. 4).

Summarizing the visual identification process, we identified a consistent pattern within the epileptogenic zone that was characterized by the combination of initial sharp transients/spikes, followed by multiband fast activity and a concurrent suppression of lower frequency activities. We display a representative contact from the resected zone from each of 15 of the patients in Supplementary Fig. 2, highlighting this pattern in both the time and time-frequency domains. Conversely, contacts outside the resected zone revealed a possible subset of these features, but not a full combination.

Downloaded from https://academic.oup.com/brain/article-abstract/141/1/117/4746664
by guest
on 08 January 2018

Automatic classification procedure and results

With the predominant features of the epileptogenic zone visually identified, we developed an algorithm to automatically extract these features from the time-frequency data. We then used machine learning methods (SVM) (Saitta, 1995) to automatically classify a contact as being inside or outside epileptogenic zone. The full details of the classification pipeline are given in the Supplementary material, sections 5 and 6. The key steps are summarized as follows.

Feature extraction

The feature extraction procedure is illustrated in Fig. 3. Detection of fast activity features uses the Frangi filter (Frangi *et al.*, 1998) for multi-scale ridge detection (Fig. 3B), followed by thresholding (Fig. 3C) and morphological cleaning (Fig. 3D). In the second row, the suppression feature is extracted using an edge-preserving guided filter (He *et al.*, 2013) (Fig. 3F). Then a fast activity-based temporal constraint was applied to ensure suppression features coincide with detected fast activity (Fig. 3G) before the final thresholding (Fig. 3H). Lastly, the pre-ictal spikes were found by taking the median of the power of the Morlet coefficients along the frequency axis for each time point in the time-frequency plot (Fig. 3I) and the local maxima are detected (indicated by small circles) as shown in Fig. 3J. Only the major local maxima are retained as the pre-ictal spike candidates (Fig. 3K) (Supplementary material, section 5).

Classification

Numerical descriptors, such as frequency, timing, area, etc., were extracted for each of the three features described

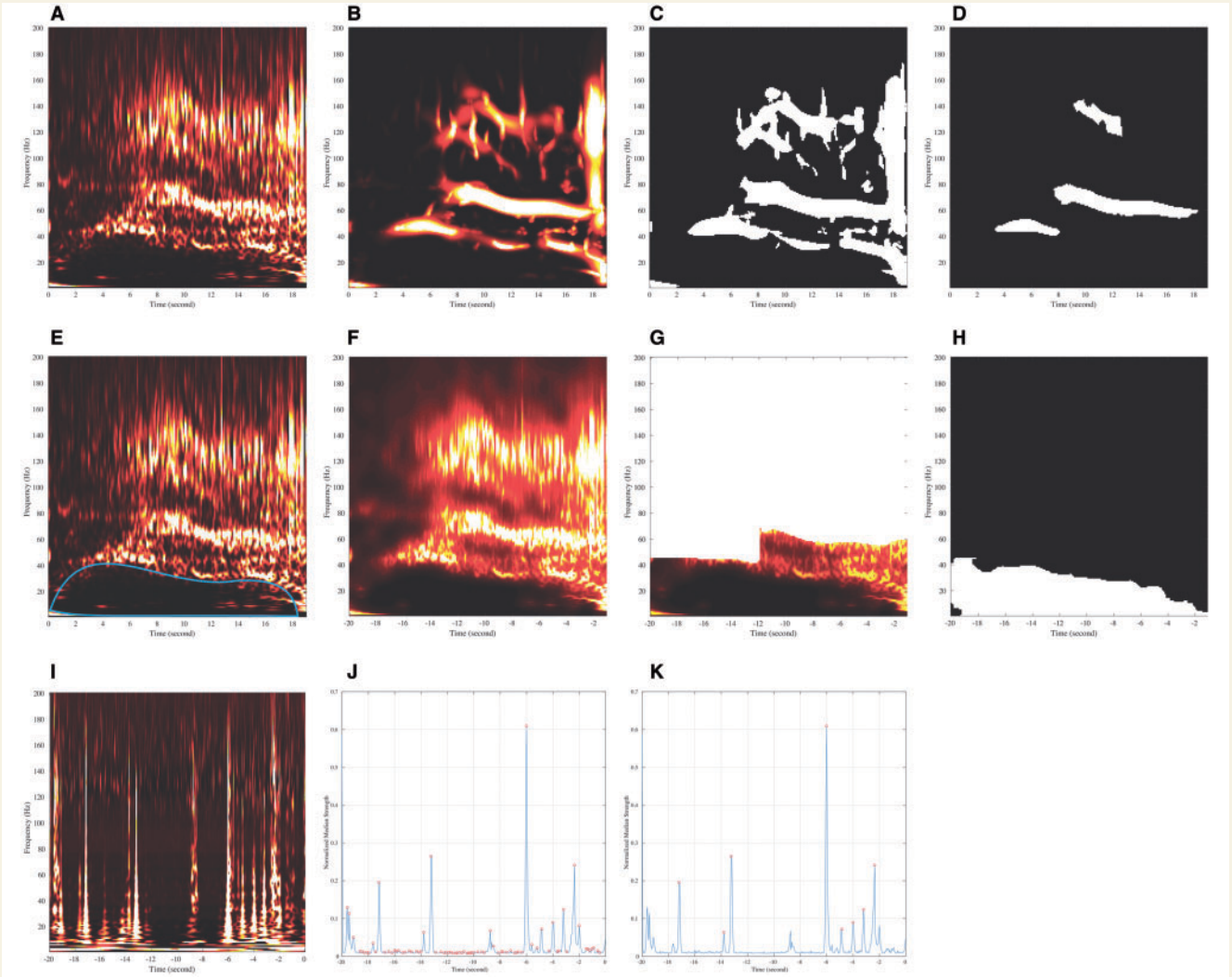

Figure 3 Illustration of feature extraction procedure. (**A–D**) Fast activity extraction. (**A**) Original post-onset time-frequency plot. (**B**) Frangi filtering result. (**C**) Thresholding result. (**D**) Final morphological cleaning result. (**E–H**) Suppression extraction. (**E**) Original post-onset time-frequency plot with ideal suppression region. (**F**) Guided filtering result. (**G**) Fast activity-based spatial constraint. (**H**) Final thresholding result. (**I–K**) Preictal spikes extraction. (**I**) Original pre-onset time-frequency plot. (**J**) Median statistics for each time point. (**K**) Small circles indicate major local maxima as the spike candidates.

Downloaded from https://academic.oup.com/brain/article-abstract/141/1/117/4746664
by guest
on 08 January 2018

above. These were then used as the input to an SVM-based classifier. During the training phase, we postulated that the epileptogenic zone was always located inside the resection region since surgery in our study population was successful. However, it is possible that epileptogenic zone contours do not exactly coincide with the resection margins. In other words, the volume of epileptogenic zone could be smaller than the volume of the resected or ablated zone. We also assume that cortical areas outside the resection region could participate in seizure propagation but did not contain any part of the epileptogenic zone. We account for the ambiguity of whether contacts in the resected regions lie in the epileptogenic zone or not by an unsupervised clustering of our combined feature descriptors to identify the subset of contact pairs in the resected zone that exhibit the three fingerprint features. The SVM model is then trained using the feature descriptors for each contact pair with the contacts labelled into two groups: epileptogenic zone (the subset of the resected regions contact pairs identified as having the desired characteristics using the unsupervised scheme) and non-epileptogenic zone (all contact pairs outside the resected regions). To avoid overfitting, a subject-based cross-validation was used. In short, we repeated the training process 17 times, in each case leaving out one subject. We then applied the classifier to identify the putative epileptogenic zone for the excluded subject. Repeating 17 times gave a classification result for each subject for each of the three observed seizures. This leave-one-subject-out cross-validation schema neither introduces bias due to the insufficient testing data as with a leave-one-sample-out approach (Varoquaux *et al.*, 2017), nor violates the data independency assumption as would be the case if we used the random split approach because our data are highly correlated between seizures within a particular subject. Finally, we applied a voting mechanism to combine the results from three seizures for each patient to generate the final classification of contacts as epileptogenic zone or not-epileptogenic zone (Supplementary material, section 6).

Results

Our goal in developing the automatic classifier was to determine whether the time-frequency patterns seen inside and outside the resection zone could indeed be used to statistically separate the two classes. The algorithm was able to objectively identify the epileptogenic zone in 15 of 17 patients. In the other two patients (Patients 6 and 16), none of the contacts were identified as epileptogenic. The total number of epileptogenic zone-identified contacts across all patients using the SVM was 64, with 58 (positive predictive value 58/64 = 90.6%) localized inside the resected area (Table 2). The program also identified 1149 contacts as not in the epileptogenic zone, of which 827 were outside the resection area and therefore assumed to be correct (false positive rate 6/827 = 0.7%). The remaining 322 contacts not identified as epileptogenic zone were found in the resection zone, but this is not surprising, since we assumed that the region of resection might be larger than the actual epileptogenic zone. We note that in one patient who underwent laser ablation surgery (Subject 4, Table 1), only two contacts were in the ablated region and that both of them were correctly classified as epileptogenic (Fig. 4). We also found that our classifier identified as epileptogenic zone most of the contacts localized inside potentially epileptogenic lesions [focal cortical dysplasia (FCD) type 2B, hippocampal sclerosis, benign tumour] (Supplementary material, section 7). The only six contacts in all patients that were identified as epileptogenic zone by the program but found outside the region of resection are shown in Fig. 4, along with all of the other correctly identified contacts.

Table 2 Result of automatic classification of the epileptogenic zone

	Prediction true	Prediction false	
Within resect	58 (TP)	322 (FN)	
Outside resect	6 (FP)	827 (TN)	0.7% (FPR)
	90.6% (PPV)		

FN = false negative; FP = false positive; FPR = false positive rate; PPV = positive predictive value; TN = true negative; TP = true positive.

As shown in Supplementary Fig. 2, most of the successfully identified contacts had a unique combination of suppression and two or more narrow frequency bands of fast activity, mostly with a preceding sharp transient (2 of 15 subjects did not have the clear pre-ictal spiking). The global similarity of the pattern across subjects could be observed very clearly, yet with some variance of the pattern.

Additional studies

To determine the uniqueness of the fingerprint model, we undertook additional studies of the fast activity and suppression and possible interactions between them, to find out if either feature by itself could differentiate epileptogenic from propagation areas.

Fast activity inside and outside the resection area

Some previous approaches to localize epileptogenic zone were based on frequency characteristics of the ictal fast activity as well as the timing of the frequency changes (Bartolomei *et al.*, 2008; David *et al.*, 2011; Gnatkovsky *et al.*, 2014). Fast activity frequency, whether or not associated with EEG flattening, was used to delineate the epileptogenic zone proposing that the regions with the earliest change and highest frequency represented 'the most epileptogenic' zone. However, the significance of fast frequencies as an absolute marker of epileptogenicity was questioned in a number of clinical studies (Blauwblomme *et al.*, 2013; Matsumoto *et al.*, 2013). To explore the

Downloaded from https://academic.oup.com/brain/article-abstract/141/1/117/4746664
by guest
on 08 January 2018

ID	Map*	TP Channel	FP Channel	ID	Map*	TP Channel	FP Channel	ID	Map*	TP Channel	FP Channel
1	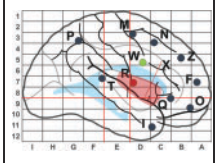	R1-R2 R2-R3 R3-R4 X1-X2 X2-X3 X3-X4 X5-X6	W2-W3 W3-W4	7	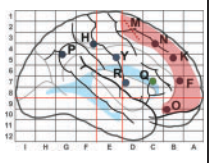	M3-M4 M5-M6 M7-M8	Q1-Q2	13	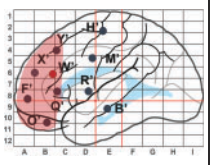	W'6-W'7	
2	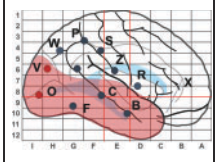	O1-O2 O2-O3 O3-O4 V1-V2 V3-V4 V4-V5 V6-V7		8	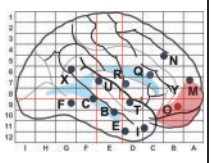	O7-O8	T1-T2	14	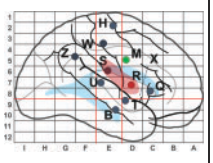	R4-R5, R5-R6	M4-M5
3	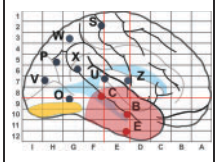	B1-B2 B2-B3 B3-B4 C2-C3 B4-B5 B7-B8 B8-B9 E1-E2 E2-E3 E6-E7		9	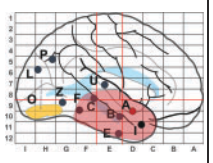	A3-A4		15	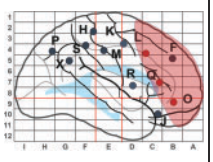	L1-L2 L2-L3 L3-L4 L4-L5 L5-L6 O3-O4 O5-O6 Q5-Q6	
4	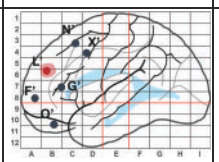	L'1-L'2 L'3-L'4 L'5-L'6		10	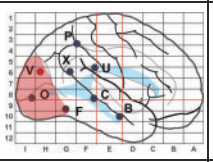	V7-V8		16	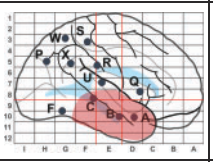		
5	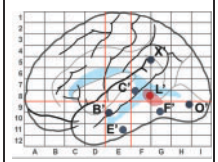	L'1-L'2		11	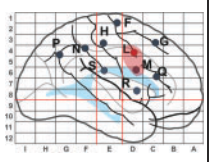	L5-L6 L6-L7 L7-L8		17	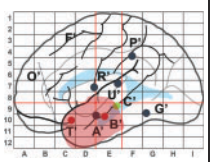	B'1-B'2 B'3-B'4 T'1-T'2 T'4-T'5 T'5-T'6 T'7-T'8 T'8-T'9	C'3-C'4
6	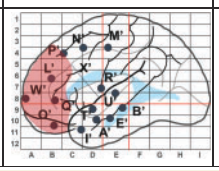			12	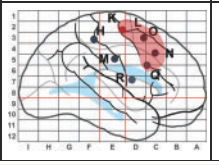	K4-K5 K5-K6 K7-K8					

Figure 4 Implantation maps with schematic representation of the resection margins (red) and bipolar SEEG channels identified by the algorithm as true positive (TP) and false positive (FP). *Electrodes on the maps are marked: (i) as red if they contain true positive (TP) channels (potentially epileptogenic inside the resection); (ii) as green if they contain false positive (FP) channels (potentially epileptogenic outside the resection); (iii) as black if they contain only true negative (TN) channels (not potentially epileptogenic outside the resection); (iv) as black in the red-shaded area if they contain false negative (FN) channels (not potentially epileptogenic inside the resection). Boundaries of prior resections are schematically shaded in yellow (only Patients 3 and 9 had a previous resection).

significance of frequency characteristics and the timing of frequency change in the identified epileptogenic zone fingerprint, we performed the following additional analyses.

First, we extracted all contact pairs exhibiting fast activity across all seizures and all subjects. We computed the maximum frequency and the timing of fast activity for each of the time-frequency plots. We then compared maximum frequency and timing of fast activity across the contacts inside the resection region with that outside the resection region, using the clinical resection labels. We further

Downloaded from https://academic.oup.com/brain/article-abstract/141/1/117/4746664
by guest
on 08 January 2018

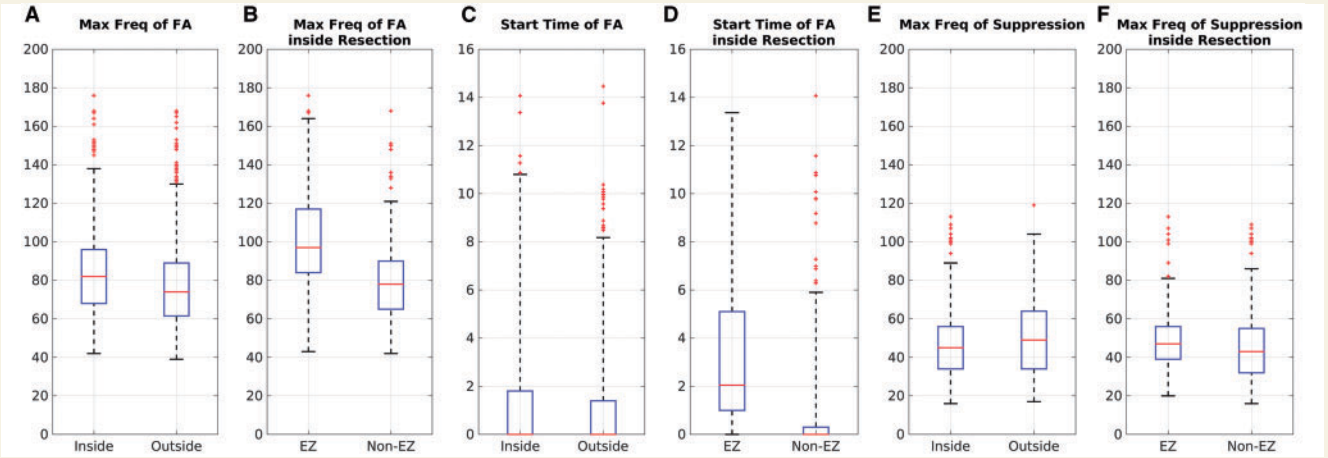

Figure 5 Boxplots of maximum frequency and timing comparison. (**A**) Maximum frequency of fast activity inside and outside resection; (**B**) maximum frequency of fast activity inside resection classified as epileptogenic zone and non-epileptogenic zone contacts. (**C**) The start time of fast activity inside and outside resection. (**D**) The start time of fast activity inside resection classified as epileptogenic zone and non- epileptogenic zone contacts. (**E**) The maximum frequency of suppression inside and outside resection. (**D**) The maximum frequency of suppression inside resection classified as epileptogenic zone and non- epileptogenic zone contacts. The boxplot spans the two central quartiles of the data around the median (red line), and the whiskers extend to a maximum of 1.5 times the box span, or to the last data point, whichever is shorter. The remaining data points are outliers. EZ = epileptogenic zone.

subdivided the contacts inside the resection region into an epileptogenic zone group and a non-epileptogenic zone group as identified by the classification procedure described above. We then compared the maximum frequency and timing of fast activity between the contacts within epileptogenic zone and those outside the epileptogenic zone.

In total (across all seizures and patients), 662 contacts (175 epileptogenic zone contacts + 487 non-epileptogenic zone contacts) with identified fast activity were localized inside the resection region and 764 contacts outside.

There is a statistically significant difference ($P = 2.26 \times 10^{-6}$ in Fig. 5A) in the population mean of the maximum frequency of fast activity across contacts within the resected region compared to those outside and also across epileptogenic zone contacts compared to non-epileptogenic zone contacts ($P = 1.02 \times 10^{-28}$ in Fig. 5B). However, the variance of the measure is sufficiently large for both cases, so that they cannot be used to differentiate between these regions using data from a single subject.

In addition to the group analysis, we undertook additional analysis for each patient individually. We found no statistically significant difference between the maximum frequency of fast activity inside the resection and that outside in 15 of 17 patients. For the other two patients, the maximum frequency of fast activity inside the resection was significantly higher than that outside for one and significantly lower for the other.

Regarding the timing of fast activity, there is no statistically significant difference ($P = 0.08$ in Fig. 5C) in the population mean of the timing of fast activity across contacts within the resected region compared to those outside. There is a statistically significant difference ($P = 2.10 \times 10^{-28}$ in Fig. 5D) across epileptogenic zone contacts compared to non-epileptogenic zone contacts. However, similar to the result of the maximum frequency of fast activity, the variance of the measure is sufficiently large that they cannot be used to differentiate between these regions using data from a single subject.

Suppression inside and outside the resection area

We used the same procedure as with the above fast activity study to also test for differences in the maximum frequency of suppression. We selected only those contacts where suppression occurred. The presence of suppression was determined by thresholding the area ratio in the time-frequency plot between the suppression region and the entire region after seizure onset. The threshold ratio used to define suppression was set to ~3.1%, which is the average ratio for the contacts inside the resection zone.

Suppression was identified in 16 of 17 patients both inside and outside the resection. In total (across all seizures and patients), suppression was found in 467 contacts (139 epileptogenic zone contacts + 328 non-epileptogenic zone contacts) inside the resection region and 474 contacts outside the resection region. We observed that highest frequency of suppression could extend into the low gamma range (Fig. 5E).

We found that there is no statistically significant difference ($P = 0.105$ in Fig. 5E) in the population mean of the maximum frequency of suppression across contacts within the resected region compared to those outside as well as across epileptogenic zone contacts compared to non-epileptogenic zone contacts ($P = 0.205$ in Fig. 5F).

Downloaded from https://academic.oup.com/brain/article-abstract/141/1/117/4746664
by guest
on 08 January 2018

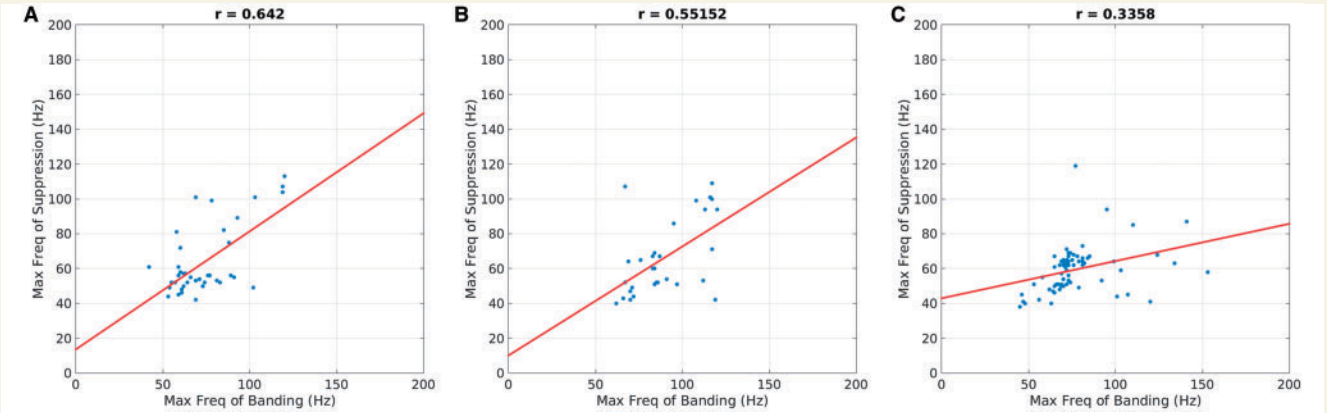

Figure 6 Scatter plot of maximum frequency of fast activity versus maximum frequency of suppression for contacts. (**A**) Classified as epileptogenic zone inside the resection; (**B**) classified as non- epileptogenic zone inside the resection and (**C**) outside the resection region. The presence of suppression was determined by thresholding 70 largest suppression areas for contacts inside the resection region and outside separately, resulting in 40 contacts in (**A**), 30 contacts in (**B**) and 70 contacts in (**C**).

The association between fast activity and suppression

To explore the relationship between fast activity and suppression, the maximum frequency of fast activity (in case where there are multiple bands, we use the maximum frequency of the lowest band as it is used as the upper bound for suppression) (Supplementary material, section 5) and the maximum frequency of suppression were extracted as described above on those contacts where both fast activity and suppression were present. We then performed a regression to study the relationship between the two maximum frequencies for contacts (i) classified as epileptogenic zone inside the resection; (ii) classified as non-epileptogenic zone inside the resection; and (iii) outside the resection region.

In contacts where both fast activity and suppression were found, we observed stronger correlation ($r = 0.642$ in Fig. 6A) between the maximum frequency of fast activity and suppression for epileptogenic zone contacts than the correlation ($r = 0.552$ in Fig. 6B) for non-epileptogenic zone contacts inside the resection. Moreover, the correlation for both epileptogenic and non-epileptogenic zone contacts, i.e. for contacts inside the resection, are much higher than that ($r = 0.336$ in Fig. 6C) for contacts outside the resection region.

The presence of suppression was determined by thresholding the k largest suppression areas for contacts inside the resection region and outside separately. Figure 6 shows results for $k = 70$. Based on bootstrap confidence intervals, we observed significant separation between the correlation of contacts inside the resection region and those outside for values of k in the range from 50 to 250, indicating the robustness of this phenomenon.

Moreover, the Dice coefficient (Dice, 1945) between the set of contacts that contained fast activity and the set of contacts that contained suppression was much larger inside the resection region (0.54) than that outside the resection region (0.27) when the same threshold ratio 3.1% is applied for determining the presence of suppression. This indicates that there is a stronger association between fast activity and suppression inside the resection region than outside.

These data suggest that suppression and fast activity might represent a combined physiological phenomenon inside the epileptogenic zone. Outside the epileptogenic zone, they are less correlated and may also appear independently due to a possible dissociated propagation of these two features.

Discussion

Defining the fingerprint of the epileptogenic zone

The time-frequency fingerprint of epileptogenic zone at seizure onset is characterized by the association of three elements: pre-ictal spikes, fast activity and suppression. A visual analysis of the time-frequency plots in a given seizure reveals this characterization. This fingerprint is reinforced by the homogeneity of this pattern across patients whatever the aetiologies and areas involved.

To automatically identify the epileptogenic zone pattern, differentiate it from the areas of propagation, and quantitatively characterize its features, we developed a SVM-based machine learning system. A novel pipeline (Supplementary material, sections 4–6) was proposed to characterize each feature in the pattern and classify each contact as being inside the epileptogenic zone or not accurately. To the best of our knowledge, this pipeline, for the first time, enables us to directly localize the epileptogenic zone, rather than merely detecting ictal/interictal spikes in SEEG recordings. Overall, the proposed algorithm could successfully identify the epileptogenic zone in a population

Downloaded from https://academic.oup.com/brain/article-abstract/141/1/117/4746664
by guest
on 08 January 2018

of patients with focal epilepsy that were seizure-free after surgery, which in turn supports our hypothesis that the time-frequency fingerprint characterizes the epileptogenic zone.

The efficacy of the detector in our selected patient population suggests that the three elements are not independent but define a pattern.

The fast activity component is structured: it is not broadband, but rather consists of multiple narrow bands. Its duration is not limited to ictal onset but may extend until the end of the seizure. Fast activity is time-related to a wide band (delta to low gamma) suppression of lower frequency activity, and the suppression cut-off frequency is correlated to the highest frequency of fast activity. The onset of fast activity/suppression is contiguous from a sharp transient (a short event characterized by a simultaneous boost of slow and fast frequencies): it can be a single spike or the last in a burst of rhythmical spikes ('pre-ictal' spikes). This transient marks the onset of fast activity (fast activity is developed from the fast component of transients) and suppression (suppression starts by interruption of the slow component of transients). The frequency contiguity between the fast component of the sharp transient and the fast activity onset is apparent in the transition from pre-ictal to ictal.

None of the three individual fingerprint elements we have identified is sufficient to characterize the epileptogenic zone, as each of these features can be identified separately, with equal or reduced intensity, at variable distances from the epileptogenic zone (fast activity without suppression or suppression without fast activity, and either with or without pre-ictal spikes). This signature likely indicates dissociated propagation of the epileptogenic zone elements. Accordingly, a strong correlation between maximum frequency of fast activity and maximum frequency of suppression was observed within the epileptogenic zone but not outside.

On the other hand, the narrow banding of fast activity in high-gamma frequencies simultaneous together with suppression in lower frequencies is indeed a peculiar pattern. Although it is apparent in most of the ictal time-frequency plots published so far, suppression (and its electrographic expression 'flattening') has to date been disregarded as a key phenomenon of ictogenicity. Often, visual analysis of SEEG can barely distinguish between very fast activity and suppression. The two distinct features can be clearly visualized using the time-frequency plots only in recent studies. Interestingly, suppression is not only limited to the lower delta frequency range but also sometimes reaches theta, beta and even the low gamma range. At the end of suppression, there is a rebound of activities in those frequencies that were previously suppressed.

The fast activity/suppression pattern is always preceded by a sharp transient. The transient waveform can be a sharp high-amplitude wave or a series of spikes with varying amplitude (often with increasing amplitude before fast activity onset). This initial short duration element is quite distinct from the slow polarizing potential underlying development of fast activity (Gnatkovsky *et al.*, 2011) but possibly could initiate it. Overt pre-ictal spikes were mainly described in association with epileptogenic lesions such as FCD type 2 and hippocampal sclerosis (Spencer *et al.*, 1992; Palmini *et al.*, 1995), but their importance has been underestimated as a general feature of focal epilepsies.

Epileptogenicity indices developed so far have taken a different approach, emphasizing analysis of fast activity, for example Bartolomei *et al.*'s (2008) energy ratio, dividing fast (beta + gamma) by slow (theta + alpha) frequency energy. Our time-frequency analysis shows that beta and low gamma are frequently suppressed, while power in fast activity is highly variable. The energy ratio mixes these two phenomena and does not account for our observation that frequency range and duration can vary both across subjects and between the epileptogenic zone and non-epileptogenic zone zones. David *et al.* (2011) localized fast activity and its early spread represented in the patient's MRI. This can be effective in some cases when the epileptogenic zone is very focal. However, we have demonstrated that there may be no significant difference between fast activity inside and outside the epileptogenic zone. Inadequacy of fast activity as an absolute marker has been documented in a number of clinical studies (Worrell and Gotman, 2011; Blauwblomme *et al.*, 2013). Gnatkovsky *et al.* (2011, 2014) measured the power of fast activity and found correlations with a slow polarizing shift to localize the epileptogenic zone. Similarly, a slow or DC component has been shown to co-localize with fast activity (Ikeda *et al.*, 1996; Thompson *et al.*, 2016).

Pathophysiological significance of the time-frequency fingerprint

The epileptogenic zone pattern can be interpreted in the light of previous work on pre-ictal/ictal transition in seizures characterized by fast activity at the onset. Correlation or functional coupling studies have shown that synchronization between neuronal populations located in distinct areas occurs before fast activity onset, during the pre-ictal spiking period (Wendling *et al.*, 2003; Bartolomei *et al.*, 2004), then de-correlation occurs throughout the entire fast activity period and synchronization increases later before seizure termination. Pre-ictal synchronicity is maximal as the slow component of the sharp transient increases in size (duration and frequency range) then disappears, whereas its fast component prolongs without interruption. During the pre-ictal period, recent microelectrode studies in human epilepsies have consistently reported a progressive increase in a rate of fast-discharging interneuronal activity while slow pyramidal activity is still present (Schevon *et al.*, 2012; Mormann and Jefferys, 2013; Truccolo *et al.*, 2014; de Curtis and Avoli, 2016; Weiss *et al.*, 2016). Then, during fast activity, acceleration of interneuronal activity

Downloaded from https://academic.oup.com/brain/article-abstract/141/1/117/4746664
by guest
on 08 January 2018

simultaneous with slowing or arrest of pyramidal activity is observed with no evidence of synchronization at the neuronal level (Truccolo *et al.*, 2014).

The narrow banding of fast activity is likely to reflect a local high frequency oscillatory activity in a homogeneous neuronal population (Ray and Maunsell, 2011; Sedley and Cunningham, 2013), and as such might correspond to increased activity of fast inhibitory interneurons modulating membrane potential of pyramidal cells (Suffczynski *et al.*, 2014). The arrest of slow paced pyramidal discharge as a consequence of fast inhibitory interneuronal activity can also explain the suppression of lower frequencies during the fast activity period (Schevon *et al.*, 2012; Truccolo *et al.*, 2014), as well as recovering of lower frequencies as fast activity ends.

The increase in fast inhibitory interneuronal activity can be caused by the decreased inhibition from slow inhibitory neurons. Several studies have shown an effect of slow inhibitory (dendritic) activity on fast inhibitory (peri-somatic) interneurons (Banks *et al.*, 2000; Pearce *et al.*, 2013). A deficient slow inhibition disinhibits fast interneurons in experimental hippocampal epilepsy (Cossart *et al.*, 2001; Khazipov *et al.*, 2004). In the neocortex, enhanced GABAergic inhibition was identified in FCD type 2 (Cepeda *et al.*, 2012).

A model of fast activity generation based on such selective deficiency of slow inhibitory processes (Stelzer *et al.*, 1994) has been elaborated by Wendling *et al.* (2002, 2010) and Bartolomei *et al.* (2004). Given a sufficient level of global excitability, the transition from pre-ictal synchronization to desynchronized fast activity can result from a brisk decrease of slow inhibition, coinciding with a concomitant increase or steadiness of fast inhibition. Comparison between simulated and real SEEG activities clearly shows that this condition can produce fast activity at seizure onset (Wendling *et al.*, 2002). Further correlations with neurobiology can be put forward based on recent papers. There is strong evidence that the parvalbumin-containing, fast-spiking basket cells are critical for gamma rhythmogenesis both *in vitro* and *in vivo*. There is also strong evidence that cortical fast-spiking interneurons are resonators, meaning that they have an abrupt onset of firing at a threshold frequency. Those features as demonstrated by Tikidji-Hamburyan *et al.* (2015) allow more robust synchronization in the presence of noise and heterogeneity. So, the spreading gamma activities inside and outside the epileptogenic zone would correspond to mechanisms different from a stochastic population oscillator. These resonator mechanisms (if operational in long-range connections) (Tomioka and Rockland, 2007) would lead to the notion of sustained fast activity projecting into a parallel propagation network thus critically challenging a classical serial view of focal seizure propagation.

In our study, we observed a multiband fast activity pattern. How could this pattern be explained? If neurons fire out of phase, their summed activity can be at a higher frequency than the discharge of any one neuron. So higher gamma activities are compatible with desynchronization between synchronized populations at the neuronal level (Kohling and Staley, 2011). Another explanation is given from the same authors: with the inhomogeneous spread, phase differences between groups of neurons, where neurons fire synchronously within each group, can result in frequency multiplication at the level of the field potential. This could also be the explanation for the existence of fast activity at similar frequencies outside the epileptogenic zone: groups of neurons firing synchronous bursts out of phase with other groups due to differences in conduction delays as activity spreads remotely from the epileptogenic zone to multiple spread relay areas in the seizure network (Proix *et al.*, 2014). Another possibility would be the coexistence of two independent generators of gamma activity. Keeley *et al.* (2017) proposed a model with multiple gamma oscillators in a single network made of two inhibitory competing subpopulations.

The current results are consistent with a new hypothesis developed by de Curtis and Avoli, (2016) on focal seizure onset mechanisms. In seizures characterized by low voltage fast activity similar to those studied in our work, they have gathered experimental evidence from animal experiments (Gnatkovsky *et al.*, 2008; Uva *et al.*, 2015) and pre-surgical microelectrode recordings in favour of a pivotal inhibitory mechanism (synchronous activation of GABA-A receptors). They propose that the same mechanism leads to an extracellular potassium increase which would facilitate seizure propagation. The importance of pre-ictal spikes (Spencer *et al.*, 1992; Spencer and Spencer, 1994; Velasco *et al.*, 2000; Gavaret *et al.*, 2004; Lagarde *et al.*, 2016) and their underlying synchronizing mechanism is also emphasized in the de Curtis-Avoli model. Their occurrence had been underestimated, possibly due to depth electrode sampling bias.

Therefore, the sequence of simultaneous events composing the time-frequency pattern that we have identified could be understood as follows. The pre-ictal spike(s) would correspond to a progressive synchronization of pyramidal cells (slow component) activating disinhibited fast somatic inhibitory interneurons (fast component). Successive bursts of fast interneuron activities would then merge into a sustained discharge (multiband fast activity) leading to pyramidal silencing (suppression). The last part of the seizure (end of suppression coinciding with fast activity decrease) could be due to local and remote post-inhibitory rebound bursting pyramidal neurons activity (Sessolo *et al.*, 2015).

The time-frequency pattern evidenced in our study reflects a summation at the local field potential level of the complex intricate neuronal mechanisms operating at seizure onset. This is presumably why its elements are inter-related. The unique combination of the three features (fast activity, suppression, and spiking) can be viewed as a fingerprint of the epileptogenic zone.

Limitations of the study

One limitation of the present study arises from the approximation in estimating the real epileptogenic zone

Downloaded from https://academic.oup.com/brain/article-abstract/141/1/117/4746664
by guest
on 08 January 2018

boundaries. We have opted for the contours of the cortical resection in seizure-free patients to delineate the area within which the epileptogenic zone lies. However, we are aware that for large resections, the epileptogenic zone is likely to be more restricted in size, and that only for very limited surgeries, such as laser ablation, will the difference between the epileptogenic zone and resected/ablated boundaries be negligible. Resection volume is an open question in epilepsy surgery where no standard based on morphological lesion is scientifically defendable. Hence the need for a biomarker is crucial.

Spatial sampling is an intrinsic restriction of any intracranial study. This limitation can also account for the variable signal-to-noise ratio of the fingerprint pattern in our patient group. A non-optimal position of the electrodes can well explain those variations. The algorithm failed to identify epileptogenic zone in two cases, and in five there were misidentified contacts. Source reconstruction methods such as minimum-norm estimation (Baillet *et al.*, 2001) could be applied to the SEEG data to potentially improve localization when the contacts do not lie directly within the epileptogenic zone.

Could this fingerprint be considered a generic trait of focal epilepsies? Its main features and putative pathophysiology are tightly related to the existence of fast activity at seizure onset. This fast activity was a patient selection criterion of the current study. Even though this is the most common electrophysiological signature (Singh *et al.*, 2015), other slower rhythmical activity patterns made of spikes or spike-and-waves have also been observed.

Acknowledgements

The authors would like to thank the following treating physicians, whose patients were included in the study: Drs Andreas Alexopoulos, William Bingaman, Nancy Foldvary-Schaefer, Stephen Hantus, Lara Jehi, Elia Pestana Knight, Norman So, Andrey Stojic, Ahsan Moosa Naduvil Valappil. The authors also thank the anonymous reviewers for their helpful comments and suggestions.

Funding

Research reported in this publication was supported in part by the National Institutes of Health under award R01NS089212 and R01EB009048. The content is solely the responsibility of the authors and does not necessarily represent the official views of the National Institutes of Health.

Supplementary material

Supplementary material is available at *Brain* online.

References

Aubert S, Wendling F, Regis J, McGonigal A, Figarella-Branger D, Peragut JC, et al. Local and remote epileptogenicity in focal cortical dysplasias and neurodevelopmental tumours. Brain 2009; 132: 3072–86.

Baillet S, Mosher JC, Leahy RM. Electromagnetic brain mapping. IEEE Signal Process Mag 2001; 18: 14–30.

Bancaud J, Angelergues R, Bernouilli C, Bonis A, Bordas-Ferrer M, Bresson M, et al. Functional stereotaxic exploration (SEEG) of epilepsy. Electroencephalogr Clin Neurophysiol 1970; 28: 85–6.

Bancaud J, Talairach J. La Stéréo-électroencéphalographie dans l'épilepsie: informations neurophysiopathologiques apportées par l'investigation fonctionnelle stéréotaxique. Paris: Masson; 1965.

Banks MI, White JA, Pearce RA. Interactions between distinct GABA(A) circuits in hippocampus. Neuron 2000; 25: 449–57.

Bartolomei F, Chauvel P, Wendling F. Epileptogenicity of brain structures in human temporal lobe epilepsy: a quantified study from intracerebral EEG. Brain 2008; 131: 1818–30.

Bartolomei F, Wendling F, Regis J, Gavaret M, Guye M, Chauvel P. Pre-ictal synchronicity in limbic networks of mesial temporal lobe epilepsy. Epilepsy Res 2004; 61: 89–104.

Blauwblomme T, David O, Minotti L, Job AS, Chassagnon S, Hoffman D, et al. Prognostic value of insular lobe involvement in temporal lobe epilepsy: a stereoelectroencephalographic study. Epilepsia 2013; 54: 1658–67.

Boonyapisit K, Najm I, Klem G, Ying Z, Burrier C, LaPresto E, et al. Epileptogenicity of focal malformations due to abnormal cortical development: direct electrocorticographic-histopathologic correlations. Epilepsia 2003; 44: 69–76.

Bragin A, Wilson CL, Staba RJ, Reddick M, Fried I, Engel J Jr. Interictal high-frequency oscillations (80-500 Hz) in the human epileptic brain: entorhinal cortex. Ann Neurol 2002; 52: 407–15.

Cepeda C, Andre VM, Hauptman JS, Yamazaki I, Huynh MN, Chang JW, et al. Enhanced GABAergic network and receptor function in pediatric cortical dysplasia Type IIB compared with Tuberous Sclerosis Complex. Neurobiol Dis 2012; 45: 310–21.

Cossart R, Dinocourt C, Hirsch JC, Merchan-Perez A, De Felipe J, Ben-Ari Y, et al. Dendritic but not somatic GABAergic inhibition is decreased in experimental epilepsy. Nat Neurosci 2001; 4: 52–62.

de Curtis M, Avoli M. GABAergic networks jump-start focal seizures. Epilepsia 2016; 57: 679–87.

David O, Blauwblomme T, Job AS, Chabardes S, Hoffmann D, Minotti L, et al. Imaging the seizure onset zone with stereo-electroencephalography. Brain 2011; 134: 2898–911.

Dice LR. Measures of the amount of ecologic association between species. Ecology 1945; 26: 297–302.

Frangi AF, Niessen WJ, Vincken KL, Viergever MA. Multiscale vessel enhancement filtering. In: Medical image computing and computer-assisted interventation—MICCAI'98. Berlin, Germany: Springer; 1998. p. 130–7.

Gavaret M, McGonigal A, Badier JM, Chauvel P. Physiology of frontal lobe seizures: pre-ictal, ictal and inter-ictal relationships. Suppl Clin Neurophysiol 2004; 57: 400–7.

Gnatkovsky V, de Curtis M, Pastori C, Cardinale F, Lo Russo G, Mai R, et al. Biomarkers of epileptogenic zone defined by quantified stereo-EEG analysis. Epilepsia 2014; 55: 296–305.

Gnatkovsky V, Francione S, Cardinale F, Mai R, Tassi L, Lo Russo G, et al. Identification of reproducible ictal patterns based on quantified frequency analysis of intracranial EEG signals. Epilepsia 2011; 52: 477–88.

Gnatkovsky V, Librizzi L, Trombin F, de Curtis M. Fast activity at seizure onset is mediated by inhibitory circuits in the entorhinal cortex *in vitro*. Ann Neurol 2008; 64: 674–86.

Gonzalez-Martinez J, Mullin J, Vadera S, Bulacio J, Hughes G, Jones S, et al. Stereotactic placement of depth electrodes in medically intractable epilepsy. J Neurosurg 2014; 120: 639–44.

Downloaded from https://academic.oup.com/brain/article-abstract/141/1/117/4746664
by guest
on 08 January 2018

He K, Sun J, Tang X. Guided image filtering. Pattern Anal Mach Intell IEEE Trans 2013; 35: 1397–409.
Ikeda A, Terada K, Mikuni N, Burgess RC, Comair Y, Taki W, et al. Subdural recording of ictal DC shifts in neocortical seizures in humans. Epilepsia 1996; 37: 662–74.
Keeley S, Fenton AA, Rinzel J. Modeling fast and slow gamma oscillations with interneurons of different subtype. J Neurophysiol 2017; 117: 950–65.
Khazipov R, Khalilov I, Tyzio R, Morozova E, Ben-Ari Y, Holmes GL. Developmental changes in GABAergic actions and seizure susceptibility in the rat hippocampus. Eur J Neurosci. 2004; 19: 590–600.
Kohling R, Staley K. Network mechanisms for fast ripple activity in epileptic tissue. Epilepsy Res 2011; 97: 318–23.
Lagarde S, Bonini F, McGonigal A, Chauvel P, Gavaret M, Scavarda D, et al. Seizure-onset patterns in focal cortical dysplasia and neurodevelopmental tumors: relationship with surgical prognosis and neuropathologic subtypes. Epilepsia 2016; 57: 1426–35.
Matsumoto A, Brinkmann BH, Stead SM, Matsumoto J, Kucewicz MT, Marsh WR, et al. Pathological and physiological high-frequency oscillations in focal human epilepsy. J Neurophysiol 2013; 110: 1958–64.
Merricks EM, Smith EH, McKhann GM, Goodman RR, Bateman LM, Emerson RG, et al. Single unit action potentials in humans and the effect of seizure activity. Brain 2015; 138: 2891–906.
Mormann F, Jefferys JG. Neuronal firing in human epileptic cortex: the ins and outs of synchrony during seizures. Epilepsy Curr 2013; 13: 100–2.
Palmini A, Gambardella A, Andermann F, Dubeau F, da Costa JC, Olivier A, et al. Intrinsic epileptogenicity of human dysplastic cortex as suggested by corticography and surgical results. Ann Neurol 1995; 37: 476–87.
Pearce A, Wulsin D, Blanco JA, Krieger A, Litt B, Stacey WC. Temporal changes of neocortical high-frequency oscillations in epilepsy. J Neurophysiol 2013; 110: 1167–79.
Proix T, Bartolomei F, Chauvel P, Bernard C, Jirsa VK. Permittivity coupling across brain regions determines seizure recruitment in partial epilepsy. J Neurosci 2014; 34: 15009–21.
Ray S, Maunsell JHR. Different origins of gamma rhythm and high-gamma activity in macaque visual cortex. PLoS Biol 2011; 9: e1000610.
Saitta L. Support-vector networks. Mach Learn 1995; 297: 273–97.
Schevon CA, Weiss SA, McKhann G Jr, Goodman RR, Yuste R, Emerson RG, et al. Evidence of an inhibitory restraint of seizure activity in humans. Nat Commun 2012; 3: 1060.
Sedley W, Cunningham MO. Do cortical gamma oscillations promote or suppress perception? An under-asked question with an over-assumed answer. Front Hum Neurosci 2013; 7: 595.
Sessolo M, Marcon I, Bovetti S, Losi G, Cammarota M, Ratto GM, et al. Parvalbumin-positive inhibitory interneurons oppose propagation but favor generation of focal epileptiform activity. J Neurosci 2015; 35: 9544–57.
Singh S, Sandy S, Wiebe S. Ictal onset on intracranial EEG: do we know it when we see it? State of the evidence. Epilepsia 2015; 56: 1629–38.
Spencer SS, Kim J, Spencer DD. Ictal spikes: a marker of specific hippocampal cell loss. Electroencephalogr Clin Neurophysiol 1992; 83: 104–11.
Spencer SS, Spencer DD. Entorhinal-hippocampal interactions in medial temporal lobe epilepsy. Epilepsia 1994; 35: 721–7.
Stelzer A, Simon G, Kovacs G, Rai R. Synaptic disinhibition during maintenance of long-term potentiation in the CA1 hippocampal subfield. Proc Natl Acad Sci USA 1994; 91: 3058–62.
Suffczynski P, Crone NE, Franaszczuk PJ. Afferent inputs to cortical fast-spiking interneurons organize pyramidal cell network oscillations at high-gamma frequencies (60-200 Hz). J Neurophysiol 2014; 112: 3001–11.
Tadel F, Baillet S, Mosher JC, Pantazis D, Leahy RM. Brainstorm: a user-friendly application for MEG/EEG analysis. Comput Intell Neurosci 2011; 2011: 8.
Thompson SA, Krishnan B, Gonzalez-Martinez J, Bulacio J, Jehi L, Mosher J, et al. Interictal infraslow activity in stereoelectroencephalography: from focus to network. J Clin Neurophysiol 2016; 33: 141–8.
Tikidji-Hamburyan RA, Martinez JJ, White JA, Canavier CC. Resonant interneurons can increase robustness of gamma oscillations. J Neurosci 2015; 35: 15682–95.
Tomioka R, Rockland KS. Long-distance corticocortical GABAergic neurons in the adult monkey white and gray matter. J Comp Neurol 2007; 505: 526–38.
Truccolo W, Ahmed OJ, Harrison MT, Eskandar EN, Cosgrove GR, Madsen JR, et al. Neuronal ensemble synchrony during human focal seizures. J Neurosci 2014; 34: 9927–44.
Uva L, Breschi GL, Gnatkovsky V, Taverna S, de Curtis M. Synchronous inhibitory potentials precede seizure-like events in acute models of focal limbic seizures. J Neurosci 2015; 35: 3048–55.
Varoquaux G, Raamana PR, Engemann DA, Hoyos-Idrobo A, Schwartz Y, Thirion B. Assessing and tuning brain decoders: cross-validation, caveats, and guidelines. Neuroimage 2017; 145: 166–79.
Velasco AL, Wilson CL, Babb TL, Engel J Jr. Functional and anatomic correlates of two frequently observed temporal lobe seizure-onset patterns. Neural Plast 2000; 7: 49–63.
Weiss SA, Alvarado-Rojas C, Bragin A, Behnke E, Fields T, Fried I, et al. Ictal onset patterns of local field potentials, high frequency oscillations, and unit activity in human mesial temporal lobe epilepsy. Epilepsia 2016; 57: 111–21.
Weiss SA, McKhann G, Goodman R, Emerson RG, Trevelyan A, Bikson M, et al. Field effects and ictal synchronization: insights from in homine observations. Front Hum Neurosci 2013; 7: 828.
Weiss SA, Lemesiou A, Connors R, Banks GP, McKhann GM, Goodman RR, et al. Seizure localization using ictal phase-locked high gamma: a retrospective surgical outcome study. Neurology 2015; 84: 2320–8.
Wendling F, Bartolomei F, Bellanger JJ, Bourien J, Chauvel P. Epileptic fast intracerebral EEG activity: evidence for spatial decorrelation at seizure onset. Brain 2003; 126: 1449–59.
Wendling F, Bartolomei F, Bellanger JJ, Chauvel P. Epileptic fast activity can be explained by a model of impaired GABAergic dendritic inhibition. Eur J Neurosci 2002; 15: 1499–508.
Wendling F, Chauvel P, Biraben A, Bartolomei F. From intracerebral eeg signals to brain connectivity: identification of epileptogenic networks in partial epilepsy. Front Syst Neurosci 2010; 4: 154.
Worrell G, Gotman J. High-frequency oscillations and other electrophysiological biomarkers of epilepsy: clinical studies. Biomark Med 2011; 5: 557–66.
Wu S, Veedu HPK, Lhatoo SD, Koubeissi MZ, Miller JP, Luders HO. Role of ictal baseline shifts and ictal high-frequency oscillations in stereo-electroencephalography analysis of mesial temporal lobe seizures. Epilepsia 2014; 55: 690–8.
Zijlmans M, Jiruska P, Zelmann R, Leijten FS, Jefferys JG, Gotman J. High-frequency oscillations as a new biomarker in epilepsy. Ann Neurol 2012; 71: 169–78.

Downloaded from https://academic.oup.com/brain/article-abstract/141/1/117/4746664
by guest
on 08 January 2018